Mapping Electric Currents around Skeletal Muscle with a Vibrating Probe

W. J. BETZ and J. H. CALDWELL

From the Department of Physiology, University of Colorado Medical School, and the Department of Molecular and Cellular Biology National Jewish Hospital, Denver, Colorado 80206

ABSTRACT A vibrating microelectrode, or vibrating probe (Jaffe and Nuccitelli, 1974), was used to map the pattern of artificially created electric currents flowing around single muscle fibers at the edge of frog cutaneous pectoris muscles. When a muscle fiber was impaled with a micropipette, a "point sink" of current was often created at the site of impalement because of injury to the cell membrane. Current, being drawn from the flanking membrane, flowed into the cell only at this point. This defined current allowed us to map the spatial resolving power of the vibrating probe by moving to different positions near the impalement site. The results suggest that under our experimental conditions the limit of resolution is a few tens of micrometers. The results were fit reasonably well by a computer model. Current was also passed through a micropipette and mapped at various positions with the vibrating probe. In this case, the current flowed to a remote reference electrode. With the current electrode in the extracellular fluid, the probe signal decayed as the inverse square of the distance, as expected. With the current electrode placed intracellularly, current was funneled along the muscle fiber axis, reflecting its cable-like properties. The signal recorded by the vibrating probe was altered accordingly, and the results could be well fit by a simple model.

INTRODUCTION

Jaffe and Nuccitelli (1974) described an instrument that is capable of measuring small electric currents that flow in the extracellular fluid around cells. The instrument consists of a vibrating metal microelectrode (vibrating probe) whose signal is processed by a lock-in amplifier, which provides a measure of the potential difference between the excursion limits of the probe tip. The vibrating probe has been used in several laboratories to characterize currents generated by different kinds of cells (Jaffe and Nuccitelli, 1977; Jaffe and Woodruff, 1979; Robinson, 1979; Stump et al., 1980; Betz et al., 1980; Foskett and Scheffey, 1982). Since the probe tip operates entirely in the extracellular fluid, there is little risk of damage to the cells from which recordings are made. Previous studies have shown that the vibrating probe operates with relatively high sensitivity and low time resolution, compared with conventional recording techniques. Any cell with a spatially asymmetric pattern of steady current sinks and sources is a candidate for study with the vibrating probe.

J. GEN. PHYSIOL. © The Rockefeller University Press · 0022-1295/84/02/0143/14$1.00

Volume 83 February 1984 143–156

In normal use, the probe (vibrating perpendicular to the cell surface) is moved alternately between a remote reference and a point close to the cell. The usefulness of the instrument depends on its ability to provide a measure of current entering or leaving the cell at each recording site near the cell. That is, the probe ideally would measure membrane current density. Quantitative information, however, is lacking on this point, because in studies to date the precise geometry of membrane current sources and sinks was not known with certainty. In the present study, we have used conventional intracellular microelectrodes to generate currents (which flowed to or from a remote reference electrode) of known amplitude and duration in edge fibers of frog cutaneous pectoris muscles. These currents were recorded at different positions adjacent to the fibers with a vibrating probe. The results show that under these conditions the probe can provide an accurate measure of membrane current density.

In addition, we have measured the signal generated by an endogenous current with a known spatial profile. This current was created simply by piercing the cell membrane with a microelectrode; the damage to the cell created a "point sink" of current at the impalement site. By mapping the currents surrounding the injury site, we were able to determine the spatial resolution of the probe.

METHODS

Simplified Theory of Operation

The vibrating probe consists of a microelectrode which is vibrated continuously in the extracellular fluid (ECF), at a frequency of several hundred hertz, with a peak-to-peak excursion of a few tens of micrometers. The voltage recorded by the probe is analyzed by a lock-in amplifier. If a steady current is flowing in the ECF, along the line of probe vibration, then the output voltage recorded by the probe will vary sinusoidally at the vibration frequency. Given the relatively small magnitude of currents generated by cells, the low resistance of the ECF, and the small vibration distance, the signal will be buried in the noise of the recording system. To extract the signal from the noise, the lock-in amplifier performs three operations on the input signal. First, it converts the signal to AC, essentially by virtue of a series capacitor at its input. Second, it rectifies the signal each half-cycle at the instant the probe passes the midpoint of its excursion. This produces net signal power above (or below) the baseline, with no change in noise contribution (if there is no special component of noise present at the vibration frequency). Third, the signal is averaged over many cycles. The output of the lock-in amplifier then provides a measure of the root-mean-square potential difference between the probe tip at its excursion limits. In practice, the signal is averaged over several hundred cycles, so that the time constant of the response to a change in input voltage is ~1 s. Thus, the probe is useful for recording only steady or slowly changing signals.

Probe Manufacture

The microelectrodes (probes) were fabricated, with minor modifications, as described by Jaffe and Nuccitelli (1974). The procedure is a modification of that described by Dowben and Rose (1953). Briefly, glass capillaries are heated and pulled to a tip diameter of ~2 μm. The following steps are performed under direct visual observation with a microforge. First, the pipette is filled with melted solder. Next, a thin layer of gold, and then a platinum ball, are electroplated on the tip. The diameter of the platinum ball (10–25 μm in these experiments) is controlled by the duration of electroplating.

The probe is electrically shielded by a film of gold, which is deposited on the pipette by vacuum evaporation, and then platinum is also electroplated on this shield. A gap of a few millimeters is left between the tip and the gold/platinum shield. The components for the vibrating probe are also available commercially (The Vibrating Probe Co., Davis, CA).

Calibration Procedure

Each time a new tip is put into service, several calibration tests are performed to determine the tip's sensitivity, noise level, and other characteristics (cf. Jaffe and Nuccitelli, 1974). These are described below. In each case, a known amount of current is delivered through a conventional micropipette and flows to an indifferent electrode several millimeters away. The probe is positioned so that it vibrates in a line passing through the tip of the current-generating pipette, unless noted otherwise.

ABSOLUTE CURRENT DENSITY Current from a point source decreases as the inverse square of the distance from the source:

$$I_x = I_o/(4\pi x^2).$$

The voltage output of the lock-in amplifier is converted to current density by the following equation:

$$I_x = 2\sqrt{2} \cdot V_x/(\rho v),$$

where I_o = total current, x = distance between current source and probe tip, I_x = current density at x, V_x = voltage output of lock-in amplifier, ρ = specific resistivity of the medium, and v = vibration distance. As shown in Fig. 1 *A*, a good fit is ordinarily obtained between the theoretical (solid line) and observed (points) current densities.

VIBRATION DISTANCE The vibration distance is controlled by the voltage applied to the piezoelectric bender element. Fig. 1 *B* shows that the recorded signal varies linearly with the vibration excursion. In most experiments, the vibration distance was 30–40 μm.

LINEARITY OF GAIN Fig. 1 *C* shows that the probe signal varies linearly with the source current magnitude (I_o) over the whole range tested, which was about four orders of magnitude and encompasses the usual working range of the probe in our experiments.

PROBE ORIENTATION The maximum signal is observed when the probe is vibrated along a line passing through the current source; virtually no signal is observed with the vibration oriented perpendicular to this line.

PHASE ANGLE OF RECTIFICATION The signal detected by the probe is amplified by a lock-in amplifier (Princeton Applied Research, Princeton, NJ) which uses a phase-sensitive detector; only signals that are of the same frequency as a reference signal and with a specified phase relationship to the reference signal will produce a net output from the amplifier. The signal used to drive the oscillation of the probe is also used as the reference signal for the amplifier. The frequency of the probe vibration is thus identical to that of the reference. However, primarily because of mechanical lags, there is a phase shift between the probe position and the reference signal. For each probe, the optimal phase is empirically determined by applying a known current in the bath and adjusting the phase of the reference to maximize the output of the amplifier.

In summary, these tests serve to ensure that the probe gives an accurate measure of current at the point of recording.

Biological Recordings

The muscle used in these experiments was the frog cutaneous pectoris and all measurements were from non-endplate regions of edge fibers. The composition of frog Ringer was (mM): 115 NaCl, 2 KCl, 1.8 $CaCl_2$, and 2.4 $NaHCO_3$. The resistance of the micropipettes was ~20 MΩ and they were filled with 4 M K acetate. The muscle was

observed with an inverted fixed-stage microscope at an overall magnification of 200. Both the microelectrode and the vibrating probe were visible in the same field of view. Recordings were stored on a dual-channel chart recorder. A computer (9845; Hewlett-Packard Co., Palo Alto, CA) was used both for digitizing the measurements and for the modeling.

RESULTS

Impalement Causes an "Injury Current"

When a fiber at the edge of the muscle was impaled with a microelectrode, the vibrating probe often immediately detected an inward current located precisely

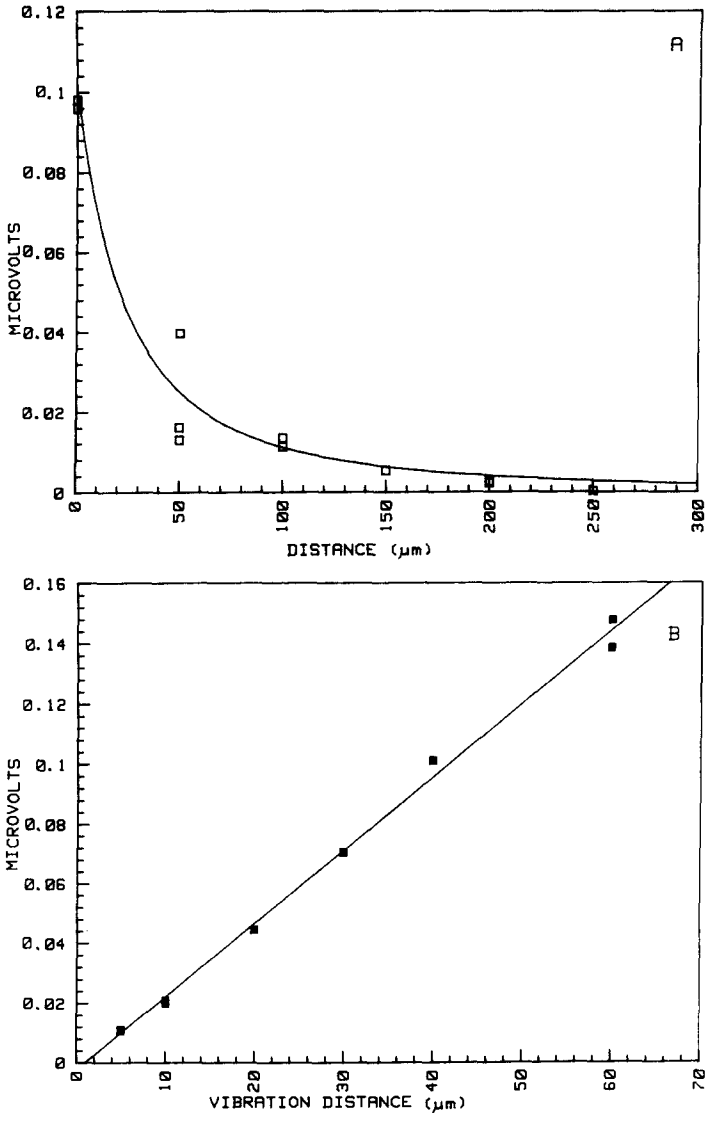

FIGURE 1.

at the impalement site. In such cases, the inward current usually declined over a period of several minutes, while the membrane potential, recorded with the intracellular microelectrode, simultaneously crept to a more negative value. These phenomena probably reflected incomplete sealing initially around the intracellular pipette, so that an injury current flowed into the cell at the site of penetration, partially shorting out the membrane potential. As the membrane gradually sealed around the pipette, the inward current declined and the membrane potential moved to a more negative value.

This injury current was useful as a means of calibrating the spatial resolving power of the vibrating probe in a biological system. This test might seem redundant, since the spatial resolution was described above, using a microelectrode as the source of current (see Methods). However, the pattern of current flow in the extracellular fluid is quite different in the two situations. With current passed through a microelectrode, current flows between it and a remote reference electrode. In the case of the injury current, extracellular currents loop from distributed membrane sources flanking the impalement site to the point

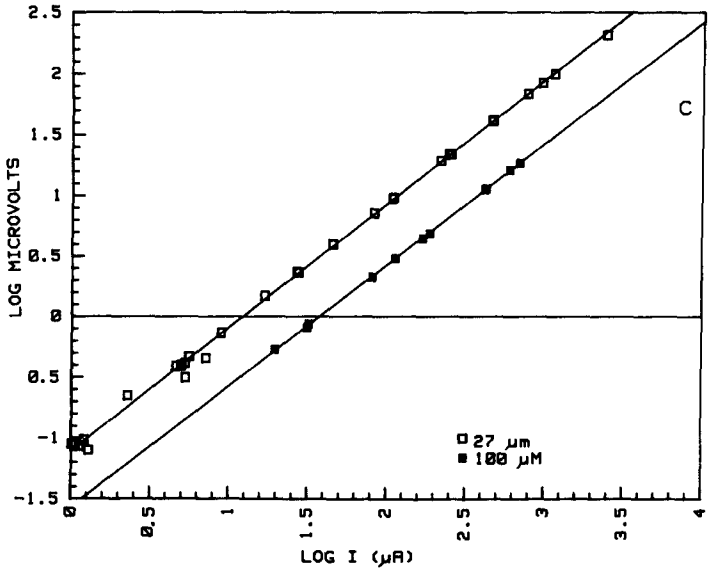

FIGURE 1. Typical vibrating probe calibration results. (*A*) Current density decays as the inverse square of distance between the vibrating probe tip and a microelectrode current source. Symbols show probe response at different distances; the line, which was constrained to pass through the first points (x near 0), is drawn according to an inverse square relationship. (*B*) Effect of probe vibration distance on the signal recorded by the probe. The voltage driving the vibrating crystal was changed, and the vibration distance and probe signal were recorded. Probe and current electrode positions and current magnitude were kept constant. The line is a linear regression through the points. (*C*) Effect of current magnitude passed through a micropipette on vibrating probe signal. Log-log plot; probe and electrode positions were fixed. Distance between microelectrode tip and probe tip = 27 μm (open squares), 100 μm (filled squares).

sink at the impalement site. The three-dimensional pattern of current flow around the cell is thus considerably different from that observed with a microelectrode as current generator.

Fig. 2 shows a current map obtained with the probe near an impalement site. (The points are fit with a line derived from a model described below.) The probe was vibrated perpendicular to the fiber axis and was moved along the fiber's lateral margin, ~35 μm from the cell. While current actually flowed into the cell only at the precise point of impalement with the microelectrode, the probe recorded inward current over a distance of ~50 μm. Thus, under these conditions, the probe output gave an overestimate of the spatial extent of the current

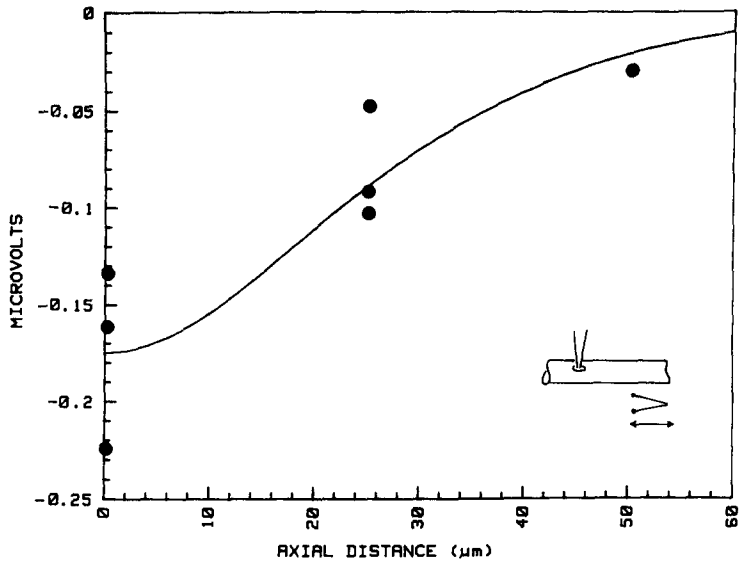

FIGURE 2. Spatial map of vibrating probe signal (y axis) recorded near an injury site caused by a microelectrode penetration. The probe was vibrated perpendicular to the muscle fiber, and was moved along the edge of the fiber (x axis), as indicated in the schematic diagram. Impalement site at $x = 0$. The radial distance between the probe and fiber was kept constant at ~35 μm. The line is drawn according to a model (see text). Negative values represent inward current.

sink. This limited resolution is caused by several factors. In particular, as currents loop from neighboring regions of the fiber and converge upon the impalement site, they acquire net inward components at points that are axially remote from the impalement site. The region in which an inward current would be detected depends on both the axial and radial distance from the impalement site. As we show below, this region is V-shaped, with its focus upon the impalement site. Since the vibrating probe measures the current at the midpoint of its vibration, it can be expected to detect inward current at points axially distant from the impalement site.

To gain a better idea of the spatial pattern of current flow surrounding a point sink caused by impalement injury, we used a computer to calculate two-dimen-

sional potential and current profiles for a simple model. We calculated the potential field surrounding a line on which was placed a number of electric dipoles. The dipoles were positioned in such a way as to mimic the biological point sink of current (Fig. 3*A*). Specifically, all negative poles were placed at $x = 0$ (the injury site), while positive poles were placed symmetrically about the center at 50-μm intervals for a distance of 3 mm along the line. To reflect the distribution of membrane current sources, the strength (I_d) of the dipoles was decreased exponentially with the distance with a length constant of 1 mm (about the same as the length constant of a muscle fiber).

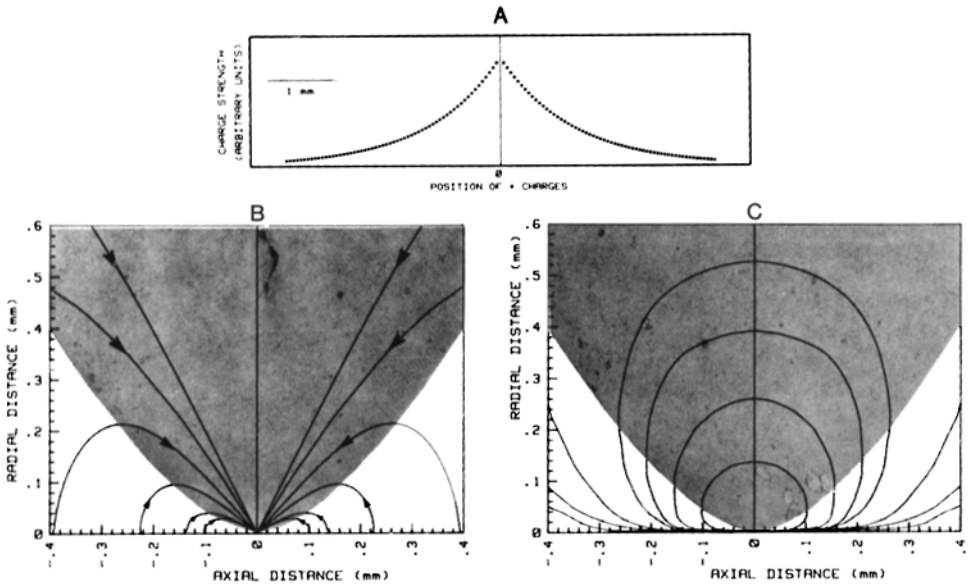

FIGURE 3. (*A*) Model used to compute current lines and isopotential lines surrounding a point sink of current in a muscle fiber caused by impalement injury. Positive charges were placed on a line at positions shown on the x axis. Each carried a charge of magnitude shown on the y axis. For each positive charge, a negative charge of equal magnitude was placed at $x = 0$. Two-dimensional current lines (*B*) and isopotential lines (*C*) were calculated from the model. In *B* and *C* the muscle fiber surface is the x axis, with the point sink at $x = 0$. The shaded areas denote the regions in which the probe, vibrating perpendicular to the muscle fiber, would record net inward current.

This is a multiple-quadrupole model. In order to calculate the potential at any given point (x, y) in space, the summed contribution of symmetrical pairs of dipoles with their negative poles superimposed (i.e., multiple quadrupoles) was calculated. The potential produced by any single quadrupole is given by:

$$V(x, y) = \frac{I_d \rho}{4\pi}\left(\frac{1}{R_{-d}} - \frac{2}{R} + \frac{1}{R_{+d}}\right)$$

where R, R_{-d}, and R_{+d} equal the distance from the given point (x, y) to the central negative pole and to the flanking positive poles at $x = -d$ and $x = +d$, respectively,

I_d = the strength of the poles, and ρ = the specific conductivity of the Ringer (80 $\Omega \cdot$cm). For each iteration, the value of d was incremented by 50 μm and I_d was decreased exponentially.

Results are shown in Fig. 3, *B* and *C*. The x axes represent the edge of the muscle fiber, with the injury site at $x = 0$, and the region in which the vibrating probe would record an inward current is shaded. Note that the further one moves away from the muscle, the greater is the axial length over which an inward current will be recorded (even though the actual membrane current is outward for all points except $x = 0$).

Fig. 3*B* shows current lines (which are also the electric field lines) looping from membrane sources to the sink. The edges of the shaded region intersect the current lines at points where they are parallel to the x axis. Fig. 3*C* shows isopotential lines; current flow is perpendicular to these lines. The margin of the shaded area (area of inward current) intersects the isopotential lines at points where they are perpendicular to the x axis. This figure illustrates the blunt shape of the region of inward current (shaded) near the injury site. That is, even at radial (y axis) distances as small as 40 μm, inward current will be detected at axial (x) positions as far as 100 μm from the point sink.

The line fitting the points in Fig. 2 is drawn from this model. That is, the inward or outward component of current was calculated for different axial distances (the radial distance was 35 μm, as in the biological experiment) and then normalized to the observed points with a single scaling factor. The theoretical curve fits the data reasonably well. It also serves to emphasize the point that although the extent of the region over which the probe measured inward current was much larger than the actual dimension of the membrane current sink (at most, a few micrometers at the impalement site), this behavior is just what one would predict around this well-defined current sink.

Thus, several features serve to limit the spatial resolution of the vibrating probe. In particular, the blunt shape of the region of inward current near the injury site (Fig. 3, *B* and *C*, shaded region) makes it especially important to use small probe tips, small vibration distances, and a close approach to a cell in order to map accurately the margins of membrane current sources and sinks.

Intracellular Current Injection

In this series of experiments, negative current was passed through the micropipette, both before and after impaling a muscle fiber. The probe was positioned near the fiber, vibrating perpendicular to its long axis. For different recordings, the probe was moved along the lateral margin of the muscle fiber. Fig. 4 shows the effects of impalement on the signal recorded by the probe. The open symbols were obtained before impalement: the signal decreased sharply over a distance of ~250 μm. After impalement (and after the injury current had decayed), the same (inward) current was passed through the micropipette. The signal recorded with the probe (filled symbols) was now greatly reduced at the impalement site, but decayed more slowly with distance, being clearly detectable at a point 1 mm along the fiber's edge. This experiment illustrates the cable-like properties of the muscle fiber. Intracellular current was funneled down the fiber axis and

leaked out through the membrane. The probe signal, reflecting the membrane current, decayed exponentially with distance.

A more quantitative analysis of this behavior was applied to several muscle fibers in an attempt to determine how accurate the probe signal is when recordings are made at any radial distance (r) and any axial distance (x) from the impalement site. In addition, the effects of impalement injury were also taken into account, insofar as some of the injected current would leak out of the cell at this site. A derivation of the equation is given in the Appendix. The equation is:

$$I_{x,r} = \frac{I_o \cdot f \cdot r}{4\pi(x^2 + r^2)^{1.5}} + \frac{I_o \cdot (1 - f) \cdot e^{-x/L}}{4\pi L(a + r)} \quad (1)$$

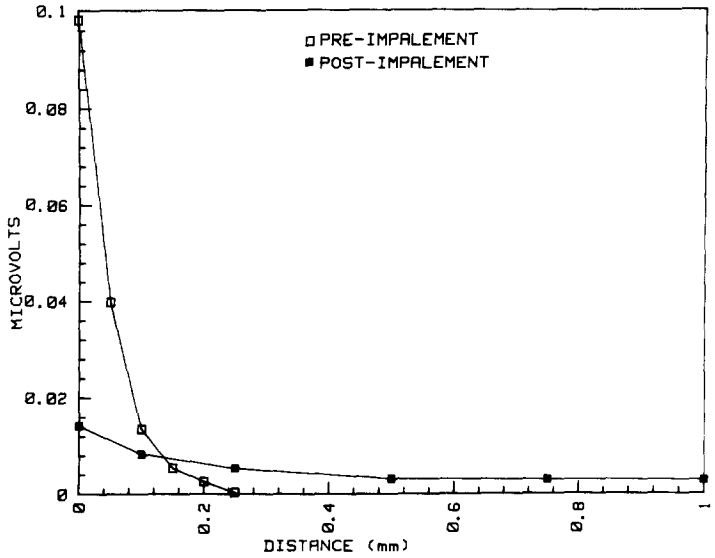

FIGURE 4. Vibrating probe signal in response to current passed through a micropipette (y axis) at different positions along the edge of a muscle fiber (x axis). The probe was vibrated perpendicular to the fiber's edge, at a radial distance of ~100 μm. The open squares were obtained with the microelectrode positioned just outside the muscle fiber, at $x = 0$. The filled squares were obtained after the microelectrode had been advanced several micrometers and had impaled the fiber.

where $I_{x,r}$ is the current density at any x and r, I_o is the injected current, f is the fraction of current escaping through impalement site, L is the length constant of the fiber, and a is the fiber radius.

There are two terms in the equation. The first describes the initial steep fall in the signal caused by current leaking through the impalement (injury) site. The second term describes the current leaking through normal pathways (ionic channels) and is derived from standard cable theory. Fig. 5 shows the results from one experiment. The probe signal (symbols) is plotted against the axial distance from the impalement site. In this experiment, the vibration distance was

35 μm, the radial distance was 125 μm, and the specific resistivity of the medium was 80 Ω·cm. There is an initial steep fall of the signal, followed by a more gradual fall. The solid line is drawn according to Eq. 1, with $I_o = 1$ nA, $f = 0.13$, $L = 1$ mm, and $a = 35$ μm. The dotted line shows the expected contribution of current leaking through membrane channels. It is clear that the probe gives an accurate measure of currents under these conditions.

DISCUSSION

As has been shown previously, the vibrating probe offers several advantages for

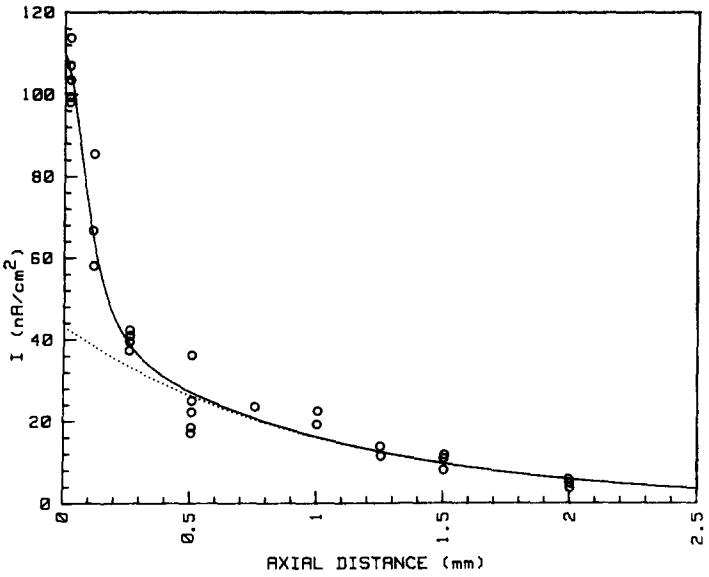

FIGURE 5. Vibrating probe response (converted to current density) to current passed through an intracellular micropipette. The x axis represents the edge of the muscle fiber. Probe vibration was perpendicular to the edge of the fiber. The solid line shows the expected current density, calculated independently according to Eq. 1. The dotted line shows the component of current due to the normal cable properties of the muscle fiber; the difference between the two curves shows the contribution of the current leaking out of the cell through the site of impalement (injury site).

the investigation of certain kinds of electrical currents. For instance, it is relatively "non-invasive," in that a cell under study is not subjected to any potentially harmful procedure, such as impalement with a microelectrode. It has a high sensitivity and can detect signals as small as ~10 nV in our hands; in mammalian Ringer's, this corresponds to a current density of ~0.1 μA/cm². (By way of comparison, bath application of acetylcholine in sufficient concentration to produce a 1-mV depolarization of a mammalian skeletal muscle fiber with an input resistance of 0.5 MΩ would generate a current density of ~200 μA/cm² at an endplate with an area of 1,000 μm².) Even smaller currents can be recorded

in solutions with higher resistivities. In addition, we have shown that the probe is capable of reasonable spatial resolution; mapping a point sink of current produced by a microelectrode impalement suggests a resolution of a few tens of micrometers. For instance, with care, the boundaries of a current generator the size of a mammalian endplate (~40 μm) could be mapped. Reducing the probe tip size and vibration distance should give even better resolution.

The vibrating probe is not suitable for some types of studies, as presently configured. There is a continual trade-off between sensitivity and time resolution. For instance, in the present study the time constant of response of the instrument was ~1 s, which clearly makes it of no use for studying fast signals, such as synaptic potentials. Also, the fact that the probe tip is constrained to vibrate in the horizontal plane makes it difficult to use on flat, isolated cells or cells grown in culture. In addition, the probe measures only that current vector along the line of its vibration, and it is necessary to rotate the probe and repeat measurements to obtain a two-dimensional map. This problem can be avoided by using a probe that moves in a circle (Freeman et al., 1981). Finally, the rather tedious procedure for manufacturing tips, combined with their fragility, requires a considerable investment to start and maintain the instrument.

In the following papers, we describe experiments in which we used the vibrating probe to identify and study an endogenous current generated by skeletal muscle fibers in their synaptic region.

APPENDIX

Inward current is injected into a muscle fiber through a micropipette and flows from a remote reference electrode. A vibrating probe, oriented perpendicular to the muscle fiber, is positioned at some point (x, r) in the extracellular fluid (x = axial distance, and r = the radial distance from the impalement site). The current density recorded by the probe is calculated below.

The current follows one of two pathways (Fig. 6). If the fiber was injured at the impalement site, some current (injury site current) will enter the fiber at this site. (Endogenous injury current looping between membrane sources and sink is ignored in this treatment; only current passed through the micropipette is considered here.) The intracellular path of the remaining current (cable current) will be determined by the cable properties of the muscle fiber. The signal recorded by a vibrating probe will be the sum of the contributions of these two currents.

Definitions

x = axial distance; r = radial distance from impalement site; a = fiber radius; L = length constant; I = total current injected; $I_{m,0}$ and $I_{m,x}$ = membrane current density at $x = 0$ and x; $I_{x,r}$ = current density in extracellular fluid at position x, r.

Cable Current

AXIAL DECAY The membrane current density at any point along a uniform cable decays exponentially:

$$I_{m,x} = I_{m,0} \cdot e^{-x/L}, \text{ where } I_{m,0} = I/2L.$$

RADIAL DECAY If the axial current density ($I_{m,x}$) were uniform, then the current density would decay radially as the inverse of the radial distance from the fiber. However,

since the membrane current is not uniform, the radial current will not decay exactly as the inverse of distance.

Consider the current emanating from any single point (p) along the length of the fiber. This current density will decay as the inverse square of the distance from the point p. The probe, at position x, r, would record a signal (I^*). The probe would not record the true current density, however (unless $p = x$), because it always vibrates perpendicular to the muscle fiber axis. In other words, the probe vibration will be "off axis" unless $p = x$. This will cause the recorded signal (compared with the true current density) to be reduced by an amount cosine A, where A is the angle between the line of probe vibration and the line between the probe tip and point p (cf. Jaffe and Nuccitelli, 1974).

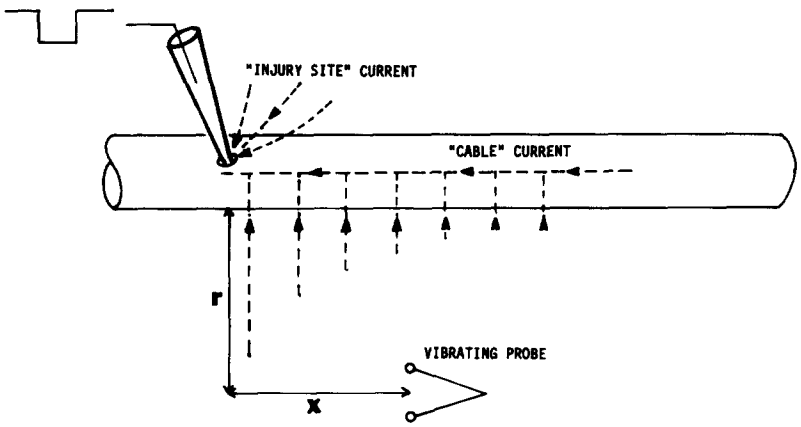

FIGURE 6. Diagram illustrating current flow for calculations in the Appendix. Current passed through an intracellular micropipette divides into two components: a cable current passes along the fiber axis and through ion channels in the membrane, as predicted by cable theory, and an injury site current leaks through the site of impalement. Each of these contributes to the signal recorded by the vibrating probe, positioned at some radial distance r and an axial distance x from the impalement site. Equations for calculating the probe's response are derived in the Appendix.

Thus, the contribution from a point will be given by:

$$I^* = \frac{I_{m,p} \cdot \cos A}{4\pi[(p - x)^2 + (r + a)^2]}.$$

The denominator reflects the inverse square decay of current density. Since $\cos A = (r + a)/[(p - x)^2 + (r + a)^2]^{0.5}$, and $I_{m,p} = (I/2L) \cdot e^{-|p|/L}$, then

$$I^* = \frac{I(r + a)e^{-|p|/L}}{8\pi L[(p - x)^2 + (r + a)^2]^{1.5}}.$$

This artificial case considers current only from a discrete point along the fiber. The total signal recorded by the probe will be the integral over all values of p. Thus,

$$I_{x,r} = \int_{-\infty}^{\infty} I^* dp.$$

This integral was evaluated by computer; the points in Fig. 7 show the results. The lines in Fig. 7 were drawn assuming that the radial current density decays simply as the inverse of the radial distance. In this case, the probe signal is given by

$$I_{x,r} = \frac{I \cdot e^{-x/L}}{4\pi \cdot L(r + a)}. \tag{2}$$

The fit of the curve to the calculated points is accurate to within a few percent (note semilog scale); thus, the simplified Eq. 2 was used to fit the data in Fig. 5.

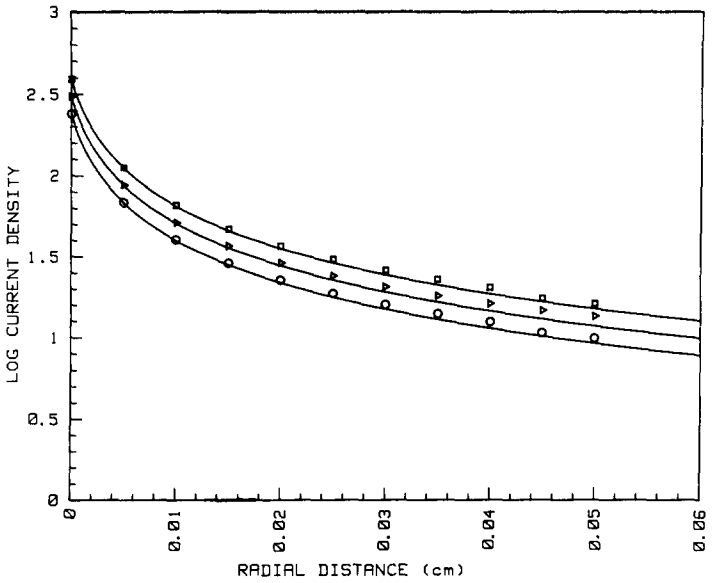

FIGURE 7. The data points show the integrals (obtained numerically by computer) of Eq. 2 (see Appendix), showing the expected decay of current density with radial distance for each of three axial distances (squares, 0 mm; triangles, 0.25 mm; circles, 0.5 mm). The lines are drawn according to a simpler equation, the assumption being that current density decays as the inverse of the radial distance from the muscle fiber. This simplified solution deviates at most by a few percent (note semilog scale) from the real situation and is used to fit the experimental data in Fig. 5.

Injury Site Current

A certain fraction (f) of the injected current will leak into or out of the fiber through the impalement site. The amount can be estimated from the amount of creep of membrane potential after impalement as the membrane seals around the electrode. For instance, if the initial membrane potential is −70 mV (at which time the probe recordings are made), and eventually the membrane potential moves to −80 mV, then the initial injury shunted one-eighth of the membrane potential (and thus one-eighth of the injected current would escape through the site).

This injury site current decays as the inverse square of the distance from the injury site. Finally, the probe will record only a portion of this current because of its off-axis alignment (unless $x = 0$).

Thus, the probe signal will be given by:

$$I_{x,r} = \frac{Ifr}{4\pi(x^2 + r^2)^{1.5}}. \quad (3)$$

The total probe signal recorded will be the sum of Eqs. 2 and 3. This is the equation (Eq. 1) used to fit experimental data illustrated in Fig. 5.

This research was supported by National Institutes of Health grants NS 10207 (to W.J.B.) and NS 16922 (to J.H.C.) and by a grant from the Muscular Dystrophy Association of America (to W.J.B.).

Received for publication 6 July 1982 and in revised form 20 October 1982.

REFERENCES

Betz, W. J., J. H. Caldwell, R. R. Ribchester, K. R. Robinson, and R. F. Stump. 1980. Endogenous electric field around muscle fibres depends on the Na/K pump. *Nature (Lond.)*. 287:235–237.

Dowben, R. M., and J. E. Rose. 1953. A metal-filled microelectrode. *Science (Wash. DC)*. 118:22–24.

Foskett, J. K., and C. Scheffey. 1982. The Cl cell: definitive identification as the salt-secretory cell in teleosts. *Science (Wash. DC)*. 215:164–166.

Freeman, J. A., J. M. Weiss, G. J. Snipes, B. Mayes, and J. J. Norden. 1981. Growth cones of goldfish retinal neurites generate dc currents and orient in an electric field. *Soc. Neurosci. Abstr.* 7:550.

Jaffe, L. F., and R. Nuccitelli. 1974. An ultrasensitive vibrating probe for measuring steady extracellular current. *J. Cell Biol.* 63:614–628.

Jaffe, L. F., and R. I. Woodruff. 1979. Large electrical currents traverse developing *Cecropia* follicles. *Proc. Natl. Acad. Sci. USA*. 76:1328–1332.

Robinson, K. R. 1979. Electrical currents through full-grown and maturing *Xenopus* oocytes. *Proc. Natl. Acad. Sci. USA*. 76:837–841.

Stump, R. F., K. R. Robinson, R. L. Harold, and F. M. Harold. 1980. Endogenous electrical currents in the water mold *Blastocladiella emersonii* during growth and sporulation. *Proc. Natl. Acad. Sci. USA*. 77:6673–6677.